23rd ABCM International Congress of Mechanical Engineering
December 6-11, 2015, Rio de Janeiro, RJ, Brazil

FLOW OF A DROP THROUGH A CONSTRICTED CAPILLARY USING LATTICE-BOLTZMANN METHOD

Mariana Luisa de Lima Torquato
Marcio da Silveira Carvalho
PUC-Rio, Department of Mechanical Engineering. Rua Marquês de São Vicente 225, Gávea. 22453-900 Rio de Janeiro, RJ, Brazil.
mlltorquato@gmail.com
msc@puc-rio.br

Raquel Quadros Velloso
PUC-Rio, Department of Civil Engineering. Rua Marquês de São Vicente 225, Gávea. 22451-900 Rio de Janeiro, RJ, Brazil.
raquelvelloso@puc-rio.br

Eurípedes do Amaral Vargas Jr.
PUC-Rio, Department of Civil Engineering. Rua Marquês de São Vicente 225, Gávea. 22451-900 Rio de Janeiro, RJ, Brazil.
vargas@puc-rio.br

Abstract. *Oil-in-water emulsions have been considered as a potential EOR method in the last thirty years. Microemulsion flow in porous medium causes an increase in pressure drop, caused by a viscous effect and by a capillary effect. This increased pressure drop represents a mobility reduction of the water phase, which contributes to a more efficient reservoir areal sweep and consequently a higher recovery factor. Using constricted capillaries as a model for the geometry of a pore throat connecting two adjacent pore bodies, experiments and numerical analysis using level-set / finite element method have already been performed in order to verify the effect of capillary geometry, flow conditions, liquid properties and drop size on the flow behavior. Lattice-Boltzmann methods, considered as a mesoscopic approach, present a good compromise between standard "top-down" and "bottom-up" approaches. With simple models describing the scattering of discrete particles confined to a lattice, it has been presented as a powerful tool for modeling multiphase flow through complicated geometries. This work describes the results of the implementation of a Lattice-Boltzmann method in modeling of a drop flow through a constricted capillary. The results are compared to experimental and numerical results available in the literature.*

Keywords: *Emulsion modelling, Lattice-Boltzmann method, EOR, Porous media*.

1. INTRODUCTION

Production performance of a petroleum reservoir depends on its efficiency in converting internal energy into production. Once primary recovery usually provides low recovery factor, secondary recovery methods are normally implemented after an initial period of depletion. More than 60% of world´s oil production comes from reservoirs under water injection (Baker *et al.*, 2015).

Typically, from 15 to 40% of the pore space are fulfilled by residual oil in a well-swept reservoir (Donaldson *et al.*, 1985). In order to improve oil recovery, Enhanced Oil Recovery (EOR) methods are implemented. Special fluids such as miscible gases or chemical products could be injected and/or thermal energy could be supplied by in-situ combustion or steam injection. Emulsion injection is classified as a chemical method of tertiary recovery (Rosa *et al.*, 2006).

EOR problems are deeply related to pore space geometry. On this microscopic level with a wide variety of pore sizes and shapes and diverse connectivity levels, inertial forces are negligible compared to viscous and interfacial forces, due to low flow velocities and low Reynolds numbers – rarely greater than the unity (Donaldson *et al.*, 1985). Beyond a critical relationship between viscous and capillary forces, trapped oil is mobilized, which could also cause additional effects of coalescence and droplet breakup.

Besides the use of emulsions in EOR, reinjection of produced water is a current trend pervading all the operators due to increasing pressure from environmental agencies, to its high environmental appeal and to its favorable economic factor (Farias, 2013).

Once the macroscopic behavior of the flow is influenced by the mechanisms operating in the micro scale of pore space, the flow of an immiscible drop immerse in continuous fluid through a straight and a constricted capillary was studied. Capillary´s geometry emulates the flow restriction imposed by pore throat in between two adjacent pores. This numerical study intends to verify the impact of emulsion´s flow, represented by a single droplet, in pore space and evaluate how flow parameters influence the flow resistance in this typical component of porous media.

Results were compared to numerical results obtained using weighted residuals applied to level-set finite element method (Roca-Reyes, 2011). Results are also compared to experimental results achieved by Olbricht and Leal (1993) and by Cobos *et al.* (2009).

Lattice-Boltzmann method was chosen for the simplicity in applying it to complex geometries and multiphasic flow. This method does not require the use of any additional method of interface tracking. It also does not present mass conversation problems, being very suitable to assess the objectives of this study. First of all, the method´s ability to correctly reproduce analytical solution of Poiseuille´s law in monophasic flow between parallel plates was evaluated in the range of imposed velocities.

1.1 Fluid Mechanics and Lattice-Boltzmann Method

Navier-Stokes equation, presented in vector form in Eq. (1), is widely used in fluid flow description. It is obtained from the basic law of conservation of linear momentum applied to a Newtonian fluid, for which there is a linear relashionship between the shear stress and the shear rate (Pritchard and Leylegian, 2011).

$$\rho_k \left[\frac{\partial \boldsymbol{u_k}}{\partial t} + (\boldsymbol{u_k} \cdot \boldsymbol{\nabla})\boldsymbol{u_k}\right] = \rho_k \mathbf{g} - \boldsymbol{\nabla} \cdot p + \mu_k \nabla^2 \boldsymbol{u_k} + \frac{1}{3}\mu_k \boldsymbol{\nabla}(\boldsymbol{\nabla} \cdot \boldsymbol{u_k}) \tag{1}$$

In Eq. (1), for each phase k, ρ is the density, μ is the dynamic viscosity, $\boldsymbol{u}$ is the velocity field, p is the local pressure and $\mathbf{g}$ is the gravity acceleration. Equation 1 with continuity equation and a thermodynamic state relation, such as $\rho = \rho(p,T)$ being T the temperature, provide a set of five coupled non-linear equations. Along with initial and boundary conditions, those equations could ideally be solved by determining $\boldsymbol{u}$, p and ρ for each coordinate (x, y, z, t). As Landau and Lifschitz (1987) stated, the state of a moving fluid is completely determined by $\boldsymbol{u}$, p and ρ.

Once this set of nonlinear equations presents analytical solution only for a few simple cases, numerous CFD methods were developed, being the most disseminated the weighted residuals method applied to Finite Element Method (FEM), Finite Difference Method (FDM) and Finite Volume Method (FVM).

Steady-state incompressible flow between parallel plates is one of the cases that present analytical solution. This case is known in literature as Poiseuille´s Flow or Poiseuille´s Law. Having both plates fixed, considering gravity negligible and imposing a pressure gradient along x direction, components u_y and u_z are null and $u = u(y)$ only from the continuity equation. From the momentum equation, $\frac{\partial p}{\partial y} = \frac{\partial p}{\partial z} = 0$. Thus, $p = p(x)$ only.

Applying the no-slip condition at each wall in the x-momentum equation, the solution is obtained as presented in Eq. (2). Each wall is placed at $y = \pm R$, being $2R$ the width between plates.

$$u_x = -\frac{1}{2\mu}\frac{dp}{dx}h^2\left(1 - \frac{y^2}{h^2}\right) = u_{max}\left(1 - \frac{y^2}{h^2}\right) \tag{2}$$

The pressure drop in this flow is given by Eq. (3).

$$\frac{\partial p}{\partial x} = \frac{\partial \tau_{yx}}{\partial y} = \mu\frac{\partial^2 u_x(y)}{\partial y^2} = -\mu u_{max}\left(\frac{2}{h^2}\right) \;\leftrightarrow\; \Delta p = -\frac{2\mu L u_{max}}{h^2} \tag{3}$$

In the last thirty years, Fluid Mechanics faced a great development with the use of CFD methods in the study of diverse areas such as biomechanics, energy and sport (Pritchard and Leylegian, 2011). One of the CFD methods developed is the family of methods denoted Lattice-Boltzmann method (LBM).

Proposed by McNamara and Zanetti in 1988 as an evolution of Lattice-gas Cellular Automata, this family of methods passed through great development since then due to its simplicity of solving complex fluid dynamic problems such as flow through complex geometries and multiphasic flow without using any interface tracking method. Level-set method, which is an example of interface tracking method, was used by Roca-Reyes (2011) in conjunction with FEM to solve a similar problem.

Other advantages of using LBM are adequate accuracy to represent micro and macro scale problems incorporating thermodynamics, simplicity to parallelize code due to local nature of collision and propagation steps and unnecessity of solving the time consuming Laplace equation at each time step (Mohamad, 2011).

In LBM, space is divided in a regular lattice and velocities are discretized in a discrete set of allowed velocities for their magnitude and direction, as depicted in Fig. 1. Each allowed velocity $\boldsymbol{e_i}$ defines a state i. Fluid is modeled as a set of particle distributions for each state i and phase k, the distribution functions $f_i^k(\boldsymbol{x}, t)$, which represent the expected number of particles of phase k at a lattice site $\boldsymbol{x}$ and time t propagating with velocity $\boldsymbol{e_i}$. After propagation, particles collide in the central node of each lattice element following simple models that describe particle scattering.

Once the fluid is modeled by particle distributions, LBM is considered as a mesoscale method, providing a good compromise between standard "top-down" approach, where the continuum is described using partial differential equations such as Eq. 1, and "bottom-up" approach or molecular dynamics, where each atom or molecule is modelled using Newton´s equations of motion (Chen *et al.*, 1994).

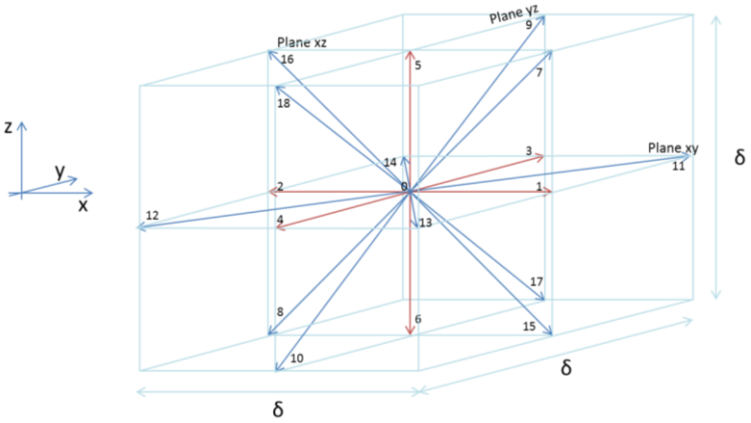

Figure 1. Diagram of one Lattice Element with its 19 lattice velocities $\boldsymbol{e_i}$, used at this study.

Numerous LBM have been proposed to simulate multiphase flows. In their annual review, Aidun and Clausen (2010) pinpoint the color-fluid model proposed by Gustensen *et al.* (1991), the interparticle-potential model proposed by Shan and Chen (1993), the free-energy model proposed by Swift *et al.* (1996), and the mean-field theory model proposed by He *et al.* (1998). The modified color-fluid proposed by Liu *et al.* (2012) is used in this study.

Boltzmann equation is discretized in time and in the directions of e_i, assuming the form of Eq. 2, where δ_t is the time step and Ω_i^k is the collision operator. Equation 2 describes the submission of each phase to collision and propagation to the next lattice site $x + e_i\delta_t$ in the next time step $t + \delta_t$ (Velloso, 2010). It is an advection equation with source term $\Omega_i^k(x,t)$, which is a function of f, being though an equation of difficult solution.

$$f_i^k(x + e_i\delta_t, t + \delta_t) = f_i^k(x,t) + \Omega_i^k(x,t) \tag{2}$$

Collision operator represents the rate of change of the particle distribution during the time interval δ_t. Tolke *et al.* (2002) described it as the combination of three suboperators, as in Eq. (3).

$$\Omega_i^k(x,t) = \Omega_i^{k(3)}\left[\Omega_i^{k(1)} + \Omega_i^{k(2)}\right] \tag{3}$$

$\Omega_i^{k(1)}$ is the Bhatnagar-Gross-Krook (BGK) collision operator, a simplified model shown in Eq. 4 that assumes that the collided particles will be relaxed toward a local equilibrium distribution, $f_i^{k,eq}$, at a constant rate $1/\tau$, where τ_k is the relaxation time of phase k.

$$\Omega_i^{k(1)} = -\frac{1}{\tau_k}\left(f_i^k - f_i^{k,eq}\right) \tag{3}$$

Equilibrium distribution function $f_i^{k,eq}$, presented in Eq. 4, is obtained through Taylor expansion of normalized Maxwell distribution function, where c is the lattice speed and w_i^k are scalar weight coefficients chosen to respect the continuity equation and the conservation of linear momentum and, as a result, responsible for capturing the macroscopic variables temperature and density.

$$f_i^{k,eq} = \rho_k w_i^k\left(1 + \frac{3}{c^2}\boldsymbol{e_i}\cdot\boldsymbol{u} + \frac{9}{2c^4}(\boldsymbol{e_i}\cdot\boldsymbol{u})^2 - \frac{3}{2c^2}\boldsymbol{u}^2\right) \tag{4}$$

Relaxation time τ_k is related to kinematic viscosity ν_k, as in Eq. (5). This equation provides the recovery of the macroscopic Navier-Stokes equations for monophasic flow.

$$\nu_k = \frac{c^2}{3}(\tau_k - \frac{1}{2})\delta_t \tag{5}$$

Tolke *et al.* (2002) proposed a linear interpolation for binary mixtures, given in Eq. (6), where R and B are the indexes used to identify the fluid phase – Red or Blue. The phase field ρ^N, defined by ρ_R e ρ_B as in Eq. (7), assumes values in the interval $[-1,1]$, being 1 when the fluid is purely red, -1 when purely blue and 0 when exactly at the interface.

$$\tau = \frac{1+\rho^N}{2}\tau_R + \frac{1-\rho^N}{2}\tau_B \tag{6}$$

$$\rho^N = \frac{\rho_R - \rho_B}{\rho_R + \rho_B} \tag{7}$$

The perturbation operator $\Omega_i^{k(2)}$ is used to generate the mixture´s interfacial region and to model the interfacial tension σ. Equations (8) and (9) provide, respectively, the operator derived by Liu *et al.* (2012) and the interfacial tension form. A_k is a free parameter used to control the interfacial tension. Liu *et al.* (2012) suggests using $A_R = A_B = A$ and $B_0 = -1/3$, $B_{1-6} = 1/18$ and $B_{7-18} = 1/36$.

$$\Omega_i{}^{(2)} = \frac{A_k}{2}\left|\boldsymbol{\nabla\rho^N}\right|\left[w_i\frac{\left(\boldsymbol{e_i\cdot\nabla\rho^N}\right)^2}{\left|\boldsymbol{\nabla\rho^N}\right|^2} - B_i\right] \tag{8}$$

$$\sigma = \frac{2}{9}(A_R + A_B)\tau c^4\delta_t \tag{9}$$

The recoloring operator $\Omega_i^{k(3)}$ proposed by Latva-Kokko and Rothman (2005) is used to promote the phase segregation and to guarantee the interface sharpness. This algorithm generates a symmetrical distribution around the interface, being responsible for reducing spurious velocity and lattice pinning problem.

$$\Omega_i^{k(3)}\left(f_i^R\right) = \frac{\rho_R}{\rho}f_i^{post-perturbation} + \beta\frac{\rho_R\rho_B}{\rho}\cos(\varphi_i)\,f_i^{eq}\big|_{u=0} \tag{8}$$

$$\Omega_i^{k(3)}\left(f_i^B\right) = \frac{\rho_B}{\rho}f_i^{post-perturbation} - \beta\frac{\rho_R\rho_B}{\rho}\cos(\varphi_i)\,f_i^{eq}\big|_{u=0} \tag{9}$$

In Eqs. (8) and (9), β is the segregation parameter, related to interface thickness and φ is the angle between $\nabla\rho^N$ and the velocity e_i, as in Eq. (10). β should be defined in the interval $[0,1]$ to assure a positive distribution function. Liu *et al.* (2012) tested β equals to 0.7 and 1.0 and verified that the higher β is, the more accurate is the interfacial tension and the higher is the spurious velocities. Liu *et al.* (2012) also concluded that $\beta = 0.7$ presents better agreement with the theoretical Taylor relationship between deformation and capillary number.

$$\cos(\varphi_i) = \frac{\boldsymbol{e_i\cdot\nabla\rho^N}}{|\boldsymbol{e_i}||\boldsymbol{\nabla\rho^N}|} \tag{10}$$

Applying continuity equation and conservation of linear momentum, macroscopic variables ρ and u are obtained, as in Eqs. (11) and (12). Macroscopic variable p is obtained from the state relation exposed in Eq. (13), where c_s^k is the speed of sound of fluid k in the lattice.

$$\rho_k = \sum_i f_i^k \tag{11}$$

$$\rho\boldsymbol{u} = \sum_i\sum_k f_i^k\boldsymbol{e_i} \tag{12}$$

$$p_k = \rho_k(c_s^k)^2 \tag{13}$$

The boundary conditions proposed by Zou and He (1997) are used in this study: half-way wall bounceback scheme for walls, imposed pressure in the exit, and imposed velocity in the entry.

1.2 Emulsion modeling and experimental results

The flow of a drop through a constricted capillary describes well the emulsion transport in porous media. This was experimentally studied by Olbricht and Leal (1983) and Cobos *et al.* (2009).

Olbricht and Leal (1993) observed that the droplet faced huge morphological alteration when flowing through the restriction, which is accompanied by an additional pressure drop when compared to flow through straight capillaries. This increase in pressure drop could be responsible for drop retention at certain conditions of pressure gradient and restriction diameter.

They also noted that the effect of tube geometry on the motion of deformable drops is strongly dependent on capillary number. For sufficiently large capillary number, drop elongation could lead to drop breakup. Effects on the drop shape are intrinsically related to viscosity ratio and capillary number.

Cobos *et al.* (2009) proposed a mobility reduction factor f calculated as in Eq. (14), used to describe the effect of partial pore blocking on the pressure drop faced by the flow. $\Delta P_{monophasic}$ is the steady pressure drop for monophasic flow and $\Delta P_{emulsion}$ is the peak pressure observed during emulsion flow.

$$f = \frac{\Delta P_{monophasic}}{\Delta P_{emulsion}} \tag{14}$$

In emulsions constituted by small drops compared to throat diameter, f does not depend on capillary number, being only a function of viscosity ratio and drop size. For large drops when compared to throat diameter, f is strongly dependent on capillary number, as observed previously by Olbricht and Leal (1993).

Roca and Carvalho (2013) presented a numerical study solved by coupling a modified level-set method to a fully-implicit finite element method. This numerical study observed the same dependence on drop size noticed in the

experimental study of Cobos *et al.* (2009). For small drops when compared to throat diameter (tested $d_{drop}/D = 0.4$), there is a weak effect on pressure drop caused by drop flow which is almost insensitive to capillary number alterations. As drop size increases, mobility reduction decreases considerably and f is strongly dependent on capillary number.

Roca and Carvalho (2013) also observed that an increase in capillary number is accompanied by an increment in mobility reduction factor f. For an infinite capillary number, mobility reduction factor f decreases as drop size ratio or viscosity ratio increase.

As demonstrated by these numerical and experimental studies, when planning to achieve a certain flow mobility reduction through emulsion injection, emulsion should be carefully designed in terms of drop size compared to throat size, viscosity ratio and interfacial tension.

2. METHODS

The algorithm presented in section 1.1 was implemented in MATLAB. Simulations were performed in a 2 lattice of 144 x 38 x 1 elements with spatial discretization $\delta_x = 2{,}78e^{-6}m$. That lattice corresponds to a control volume of length 0,4 mm and width of 0,1 mm, which are the same dimensions used in Roca-Reyes (2011).

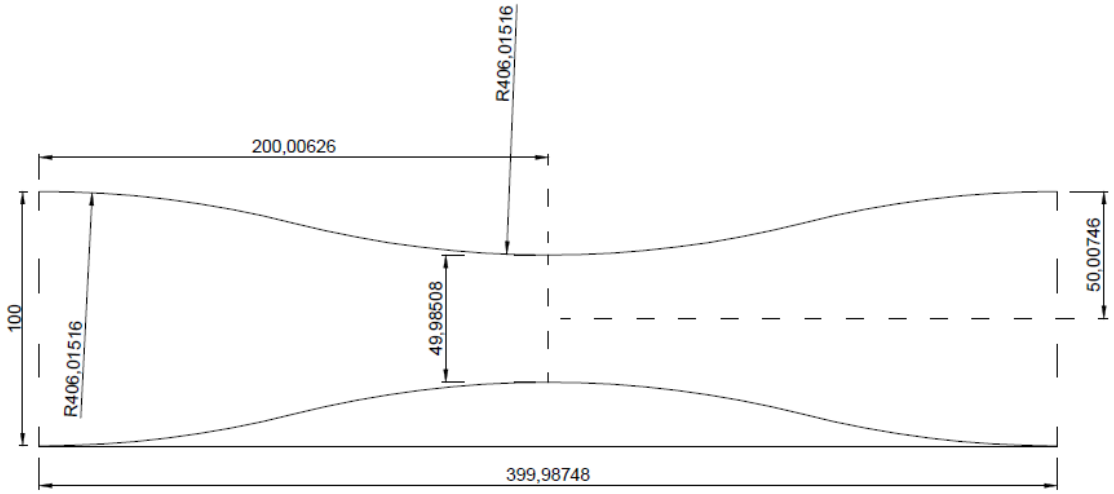

Figure 1. Control volume used in simulations with units expressed in μm.

Roca-Reyes (2011) used an axisymmetric geometry, while in this study it is used one longitudinal section from geometry of infinite parallel plates. Simulation performed is a pseudo-2D simulation, once it is applied the formulation for three dimensional flow (lattice D3Q19) to a lattice with unitary third dimension.

It is used time discretization equal to spatial discretization, $\delta_t = 2{,}78e^{-6}s$. By imposing$\delta_t = \delta_x$, the lattice velocity c is equal to unity and so the majority of equations can be simplified.

Fluid has density of 1000 kg/m3 and dynamic viscosity μ of 0,001004 Pa.s, which is the water viscosity at atmospheric pressure and temperature of 20ºC. Once the density in LBM units is equal to 1, the mass conversion factor is $\delta_m = 2{,}14e - 14\ kg$. Relaxation time τ equivalent to μ, δ_x, δ_t and $\delta_m$is 1.58432.

The control volume is initialized with unitary fluid density. The parabolic velocity field, $u_x = u_{max}\left(1 - \frac{y^2}{h^2}\right)$, is imposed in the entry and an unitary fluid density is imposed in the exit.

3. RESULTS

There are some restrictions when applying LBM to describe a multiphasic fluid flow:

- It is impossible to apply null pressure in simulation, which signifies imposing null density to the fluid, once it causes serious instabilities. In this study, focus will be done to relative pressure drop, not to absolute pressure;
- Restrictions in applying high viscosities, once it is imposed in the simulation through the parameter τ, which has limited allowed range $[0.5, 20]$ according to Zou and He (1997).

In a first step of verification, the monophasic flow between parallel plates was tested. As presented on item 1.1, this case, known as Poiseuille´s law, has analytical solution.

There is a good agreement between simulated and calculated pressure drop when the maximum imposed flow velocity is up to 0.045 m/s. Error is restricted to 3.19%. For higher velocities, the linear relationship between flow rate and pressure drop is no longer observed. This result is related to the imposition of velocities of high magnitude - near

0.1 m/s or 0.1 LBM units. LBM is a method of artificial compressibility which presents restrictions about maximum velocity and Mach number. Velocity should be kept in the order of 0.1 to reduce simulation errors (Mohamad, 2011).

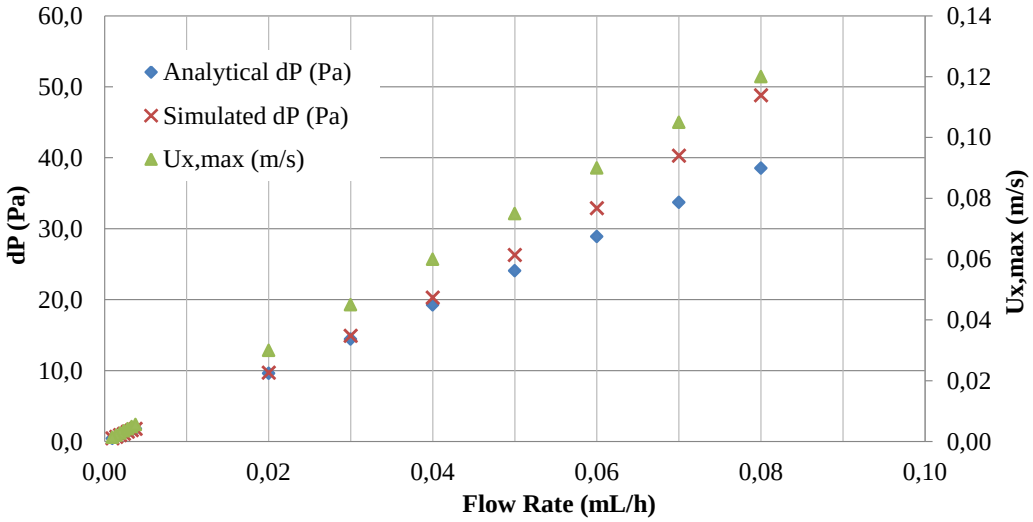

Figure 2. Comparison between analytical (blue) and simulated (red) pressure drops for different maximum velocity (green) and flow rate

Parabolic velocity profile is reproduced in all x sections of the control volume. With this experiment, it is concluded that boundary conditions were correctly been inserted in the simulation and also that the spatial and temporal discretization used were adequate.

LBM presents an initial oscillatory period due to the nature of particle propagation in the lattice. Although the magnitude of oscillation is directly related to the magnitude of the imposed velocity, there is no expressive variation in the duration of the transient period. The initial transient period stabilizes in 2.900 time steps for the monophasic flow, which is equivalent to 1 hour of computation using the algorithm programmed in MATLAB.

For the biphasic flow, the stabilization is achieved after 3.150 time steps. Higher pressure values observed in the beginning of simulation are due to the intersection of the drop with the entry section. The insertion of a drop with different viscosity and interfacial tension influences the pressure field in the flow, although it does not affect the pressure drop significantly in steady state period, as seen in Fig. 3a. After 4.000 time steps, simulated pressure drop for the monophasic and biphasic flow were, respectively, of 1.81 Pa and 1.92 Pa. Theoretical pressure drop is 1.82 Pa.

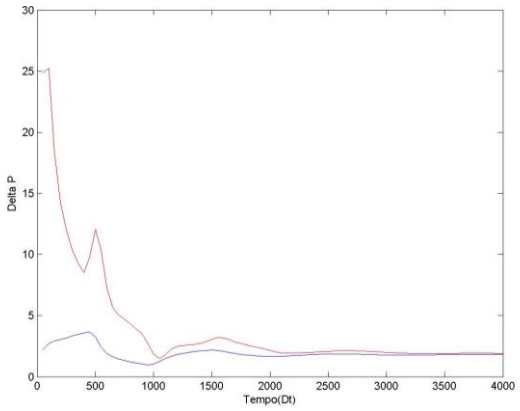

a. Monophasic (blue) and biphasic (red) flow through straight microcapillary

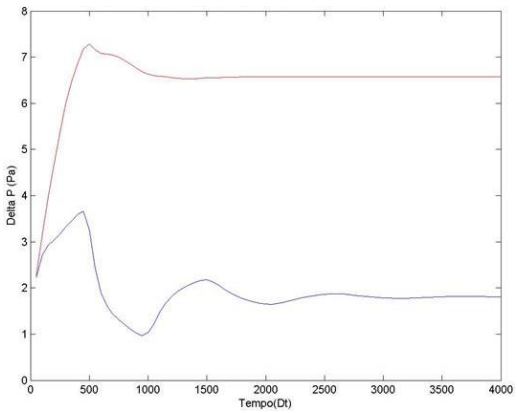

b. Monophasic flow through straight (blue) and constricted microcapillary (red)

Figure 3. Pressure drop (in Pa) in the central line of the section during simulated time in time steps

An initial transient period is also observed in the flow through constricted capillary, which is the time necessary for the velocity field to stabilize in the control volume. The introduction of the restriction leads to a faster stabilization. Steady state period is achieved after only 2.900 time steps. As it can be seen in Fig. 3b, pressure drop is much higher for the constrict capillary, 6,57 Pa, when compared to straight capillary.

In order to obtain stabilization of the initial transient period before the flow starts to be influenced by the drop entrance through the restriction, the control volume had its length augmented in 50 lattice elements. This measure was also adopted to avoid border effects related to the intersection of the dispersed drop with the entry section, which affects the pressure distribution in the beginning of the simulation. With this new 194 x 38 x 1 mesh, the drop center was moved 8 units away from the entry section. Simulation of 30.000 time steps required 13h 4 min of computational time.

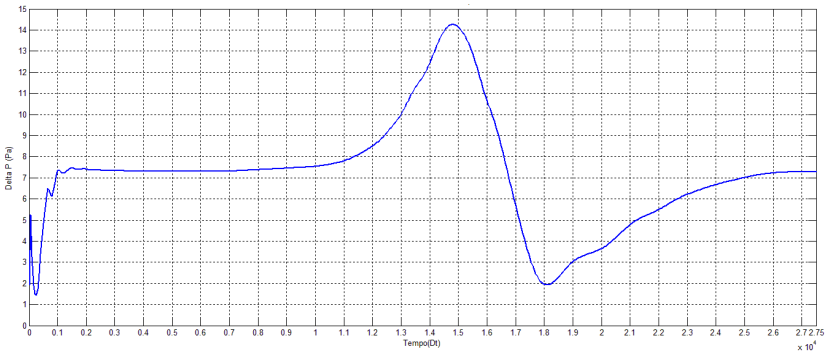

Figure 4. Pressure drop (in Pa) in the central line of the section during simulated time in time steps

Figure 4 shows qualitatively the same pressure drop signature presented by Roca-Reyes (2011) and Cobos *et al.*(2009). An increment of pressure drop is observed when drop starts the deformation process while entering the section with reduced diameter. At 14.750 time steps, drop is in its highest deformation with its first half occupying the most restrict section. With maximum superficial area per volume, an additional pressure is required to resist high interfacial force that opposes to deformation. Parameters used: $u_{x,max} = 0{,}005659 m/s$, $Re = 0{,}56$ e $Ca = 0{,}0058$.

From time step 16.750, pressure drop achieves values inferior to that observed after stabilization of transient period. Some hypothesis have been raised to explain this difference: LBM common oscillations could be occurring during the transient passage to expansion period; propagation of low pressure points in drop extremities caused by high interfacial tension and recoloring algorithm (Fig. 5). Olbricht and Leal (1993) demonstrated this great morphological alteration when flowing through the restriction as depicted in Fig. 5. Olbricht and Leal (1993) also presented a similar behavior of low or negative pressure drop after the peak, which was explained by the interactions of the mechanisms: disturbance of flow by the drop, drop deformation, interactions drop-wall and replacement of fluid of different viscosity.

a. T = 12850 Dt b. T = 15000 Dt

Figure 5. Pressure distribution of the red phase (in LBM units) in control volume

By reducing velocity, viscous forces prevail even more on inertial forces, but it also causes interfacial forces to prevail over viscous forces. When reducing velocity to 1% of original velocity, drop stabilized inside the restriction.

Same pressure drop signature was observed when using a Ca of the same order from that used by Roca-Reyes (2011), which was possible by reducing interfacial tension to 10% of its original value. More than that, a good agreement was found for mobility reduction factor f between this study ($f = 0{,}84$) and previous stud ($f = 0{,}88$).

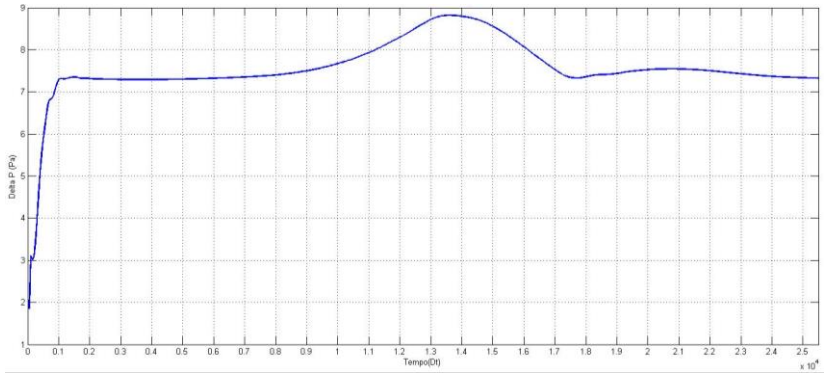

Figure 6. Pressure drop (in Pa) in the central line of the section during simulated time in time steps

Additional and more general studies in full 3D tube geometry are in progress.

4. ACKNOWLEDGEMENTS

M. L. L. Torquato was supported by PUC-Rio through an exemption scholarship.

5. REFERENCES

Aidun, C.K., Clausen, J.R., 2010. "Lattice-Boltzmann Method for Complex Flows". *Annual Review of Fluid Mechanics*, Vol.42, p.439-472.

Baker, R.O., Yarranton, H.W., Jensen, J., 2015. *Practical reservoir engineering and characterization.* Gulf Professional Publishing, Elsevier, Oxford, 1st edition.

Chen, S., Doolen, G.D., Eggert, K.G., 1994. "Lattice-Boltzmann Fluid Dynamics: A Versatile Tool for Multiphase and Other Complicated Flows". *Los Alamos Science*, n.22, p. 99-111.

Cobos, S., Carvalho, M.S., Alvarado, V., 2009. "Flow of oil-water emulsions through a constricted capillary". *International Journal of Multiphase Flow*, Vol. 35, p. 507-515.

Donaldson, E.C., Chilingarian, G.V., Yen, T.F., 1985. *Enhanced Oil Recovery, I: Fundamentals and Analyses.* Elsevier, New York, 1st edition.

Farias, M.L.R., 2013. *Recuperação avançada de óleos pesados por injeção de emulsões diluídas de óleo em água.* Ph.D. thesis, PUC-Rio, Rio de Janeiro.

Gustensen, A.K., Rothman, D.H., Zaleski, S., Zanetti, G., 1991. "Lattice Boltzmann model of immiscible fluids", *Phys. Rev. A*, vol. 43, p. 4320-4327.

He, X., Chen, S., Doolen, G.D., 1998. "A novel thermal model for the lattice Boltzmann method in incompressible limit". *J. Comput. Phys.*, Vol. 146, p. 282-300.

Landau, L.D., Lifschitz, E.M., 1987. *Fluid Mechanics (Volume 6 of Course of Theoretical Physics).* Translated by: Sykes, J.B., Reid, W.H., Pergamon Press, New York, 2nd English edition revised.

Latva-Kokko, M., Rothman, D.H., 2005. "Diffusion properties of gradient-based lattice Boltzmann models of immiscible fluids". *Physical Reviel E*, Vol.71, 056702.

Liu, H., Valocchi, A.J., Kang, Q., 2012. "Three-dimensional lattice Boltzmann model for immiscible two-phase flow simulations". *Physical Review E,* Vol. 85, 046309.

Mohamad, A.A., 2011. *Lattice-Boltzmann Method Fundamentals and Engineering Applications with Computer Codes.* Springer, London, 1st edition.

Olbricht, W.L., Leal, L.G., 1983. "The creeping motion of immiscible drops through a converging/diverging tube". *Journal of Fluid Mechanics*, Vol. 134, p. 329-355.

Pritchard, P.J., Leylegian, J.C., 2011. *Fox and McDonald´s Introduction to Fluid Mechanics.* John Wiley & Sons, New Jersey, 8th edition.

Roca-Reyes, J.F., 2011. *Análise numérica do escoamento de emulsões através de capilares retos e capilares com garganta.* MSc. thesis, PUC-Rio, Rio de Janeiro.

Roca, J.F., Carvalho, M.S., 2013. "Flow of a drop through a constricted microcapillary". *Computers & Fluids*, Vol. 87, p. 50-56.

Rosa, A.J., Carvalho, R.S., Xavier, J.A.D., 2006. *Engenharia de reservatórios de petróleo.* Editora Interciência, Rio de Janeiro, 1st edition.

Shan, X., Chen, H., 1993. "Lattice Boltzmann model for simulating flows with multiple phases and components". *Physical Review E,* Vol. 47, p. 1815-1819.

Swift, M.R., Orlandini, S.E., Osborn, W.R., Yeomans, J.M., 1996. "Lattice Boltzmann simulations of liquid-gas and binary fluid systems". *Physical Review E*, Vol. 54, p. 5041-5052.

Tolke, J., Krafczyk, M., Schulz, M., Rank, E., 2002. "Lattice Boltzmann simulations of binary fluid flow through porous media*". Philosophical Transactions of The Royal Society A*, Vol. 360, p. 535-545.

Velloso, R.Q., 2010. *Simulação numérica de problemas de acoplamento fluidomecânico em meios porosos utilizando o Método de Elementos Discretos*. Ph.D. thesis, PUC-Rio, Rio de Janeiro.

Zou, Q., He, X., 1997. "On pressure and velocity boundary conditions for the lattice Boltzmann BGK model". *Physics of Fluids*, Vol. 9, p. 1591-1598.

6. RESPONSIBILITY NOTICE

The authors are the only responsible for the printed material included in this paper.